2-1-2012

Cantilever-Based Optical Interfacial Force Microscopy

Byung I. Kim
Boise State University

6

Cantilever-Based Optical Interfacial Force Microscopy

Byung I. Kim
Department of Physics, Boise State University, USA

1. Introduction

Atomic force microscopy (AFM) is one of the most important tools that lead current nanoscience and nanotechnology in many diverse areas including physics, chemistry, material engineering, and nano-biology. The current AFM technique has been routinely applied to forced unbinding processes of biomolecular complexes such as antibody-antigen binding, ligand-receptor pairs, protein unfolding, DNA unbinding, and RNA unfolding studies (Butt et al., 2005; Fritz & Anselmetti, 1997; Schumakovitch et al., 2002). AFMs have also been applied to intermolecular friction studies (Carpick et al., 1997; Colchero et al., 1996; Fernandez-Torres et al., 2003; Goddenhenrich et al., 1994; Goertz et al., 2007; B.I. Kim et al., 2001; Major et al., 2006). These previous techniques of measuring friction employed a lateral modulation of the sample relative to the cantilever as a means to measure normal force and friction force at the same time (Burns et al., 1999a; Carpick et al., 1997; Colchero et al., 1996; Goddenhenrich et al., 1994; Goertz et al., 2007; Major et al., 2006).

However, AFM usage has been limited to passive applications (e.g., pull-off force measurement in the force-distance curve) and can only be applied to the measurement of friction while the tip is touching the sample surface because of an intrinsic mechanical instability of the tip-sample assembly near a sample surface called the "snap-to-contact problem"(Burnham, 1989; Lodge, 1983). During measurements, the mechanical instability occurs when the force derivative (i.e., dFa/dz), in respect to the tip position (z), exceeds the stiffness of the cantilever (spring constant k) (Greenwood, 1997; Israelachvili & Adams, 1978; Noy et al., 1997; Sarid, 1991), causing data points to be missed near the sample surface (Cappella & Dietler, 1999). This has been a significant barrier to understanding the nanoscopic water junction between the tip and the surface in ambient conditions, which makes it difficult, with AFM data, to directly reveal the interfacial water structure and/or analyze it with existing theories.

A decade ago for the purpose of avoiding the mechanical instability in measuring intermolecular forces, magnetic force feedback was implemented in AFM systems by attaching a magnet to the end of a cantilever (Ashby et al., 2000; Jarvis et al., 1996; A.M. Parker & J.L. Parker, 1992; Yamamoto et al., 1997). However, the magnetic force feedback requires a tedious process of attaching magnets to the backside of the cantilever using an inverted optical microscope equipped with micromanipulators (Ashby et al., 2000;

Yamamoto et al., 1997) and has poor performance in the servo system due to eddy currents (Jarvis et al., 1996; Parker & Parker, 1992; Yamamoto et al., 1997).

Interfacial force microscopy (IFM) was developed fifteen years ago, as an independent approach to avoid the mechanical instability problems related to the snap-to-contact problem associated with regular AFMs, (Chang et al., 2004; Joyce & Houston, 1991; Houston & Michalske, 1992). The IFM did not use the AFM platform, such as cantilever and optical detection schemes in measuring forces between two surfaces. Instead, the IFM uses its own force sensor with a larger tip (typical diameter around 0.1 μm to 1 μm) and an electrical detection scheme. Using force feedback, the IFM is capable of preventing the mechanical instability of the tip-sample assembly near a sample surface.

The IFM has greatly expanded applicability to the various problems at interfaces that the AFM cannot offer. IFM has been applied to diverse interfacial research including nanotribology (Burns et al., 1999b; Kiely & Houston, 1999; H.I. Kim & Houston, 2000), interfacial adhesion (Bunker et al., 2003; Huber et al., 2003) and probing of interfacial water structures (Major et al., 2006; Matthew et al., 2007). IFMs have contributed to molecular scale understanding of various surface phenomena. Kim and Houston applied IFM to measure friction force and normal force simultaneously to study the molecular nature of friction independently (H.I. Kim & Houston, 2000). The friction force is decoupled from normal force in the frequency domain. They used small vibrations to reduce the amount of wearing, getting friction information directly from the response amplitude with a lock-in amplifier. The earlier approach using AFM by Goodenhenrich et al. is similar to friction measurements but cannot be applied to friction studies at attractive regimes (Goodenhenrich et al., 1994). As an approach to study attractive regimes, friction forces have been measured using the IFM (Joyce & Houston, 1991), where the force feedback makes it possible. (Burns et al., 1999a; Goertz et al., 2007; Major et al., 2006). Burns et al. applied IFM to measure friction force and normal force simultaneously to study the molecular nature of friction to investigate the intermolecular friction along with normal forces in the attractive regime (Burns et al., 1999a).

However, the IFM technique has not been widely used due to low sensitivity and the technical complexity of the electrical-sensing method. The current IFM system uses a relatively bigger tip with the typical diameter around one micrometer for measurement of molecular interactions due to the existing low sensitivity issue in the electric force detection method of the current "teeter-totter" type of IFM force sensor (Joyce & Houston, 1991). The larger tip and the complexity of the electrical detection measurements have limited the use of the IFM as a popular tool to address the issues, especially at the single molecular level.

By combining a conventional IFM and AFM-type cantilever and its optical detection scheme, we recently developed a force microscope called the cantilever-based optical interfacial force microscope (COIFM) (Bonander & B.I. Kim, 2008). The COIFM substantively improved the force sensitivity, measurement resolution and accuracy over the conventional IFM and ordinary AFM measurements. In this chapter, the design and development of the COIFM are described along with a general description of avoiding the cantilever instability by using force feedback when measuring intermolecular forces. We derived how the interfacial force can be incorporated into the detection signal using the Euler equations for beams. Relevant calibration methods and approaches are covered for the analysis of the COIFM data. The

COIFM's unique force profiles related to ambient water structure on a surface have been demonstrated (Bonander & B.I. Kim, 2008; B.I. Kim et al., 2011). At the end of the chapter, the future applications of the COIFM system are discussed.

2. Design and development of COIFM

A schematic diagram of the overall COIFM system with the force feedback control is shown in **Figure 1(a).** We modified a commercially available AFM system (Autoprobe LS, Park Scientific Instruments, Sunnyvale, CA), which was originally designed for general purpose use of AFM, for the base of the COIFM system to be built upon. The feedback loop was developed using an RHK SPM 1000 controller (RHK Technology, Inc., Troy, MI). The feedback control parameters, such as time-constant and gain, can be manually adjusted for the optimal feedback condition. The tip-sample distance in the z-direction was controlled by a high-voltage signal controller sent to the piezo tube. An optical beam deflection detection scheme in the AFM head of an AutoProbe LS (former Park Scientific Instruments) was used to transmit the interaction force between the tip and the surface into the electrical signal (E. Meyer et.al, 1988). The wavelength of the laser light for the optical detection is 670 nm and the position-sensitive detector is a bi-cell silicon photo-diode. The head was interfaced with an RHK SPM 1000 controller, and all data presented here were recorded through analog digital converter inputs of the controller and its software. Before experimentation, the laser beam was aligned on the backside of the cantilever and A-B was adjusted to make the laser incident zero by reflecting in the middle of the photo-diode. The zero force was set as the V_{A-B} value at large separations between the two surfaces before measurement. The tip-sample distance was controlled by moving the piezo tube in the z-direction using the high-voltage signal controller.

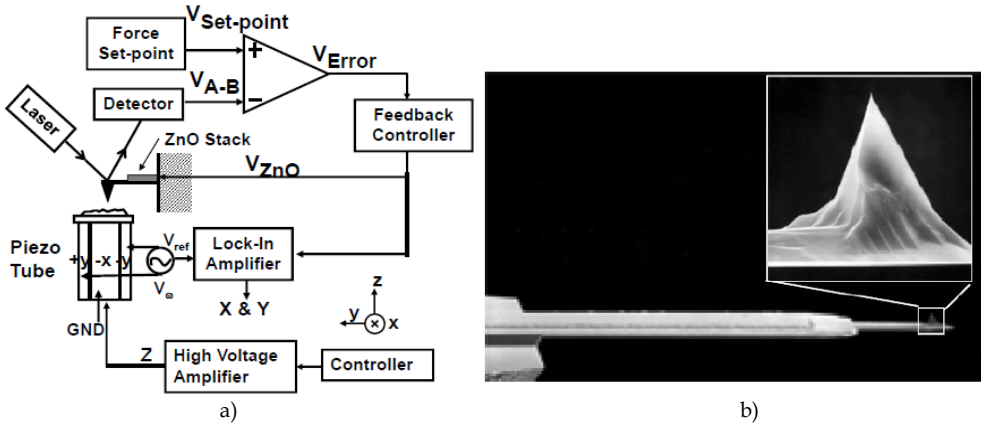

Fig. 1. **(a)** A schematic diagram of the COIFM with voltage-activated force feedback using an optical beam deflection detection method. The system consists of an LS AutoProbe AFM with a dimension micro-actuated silicon probe (DMASP) tip interfaced with an RHK SPM100 controller. The lock-in amplifier is used to measure the response amplitude.
(b) Image of the DMASP tip used for COIFM. (Courtesy of Bruker Corp.)

The tip then approached the sample until touching, using the stepping motor of the piezo tube. The tip-speed was controlled by the built-in digital-to-analog converter of the RHK controller in conjunction with the high-voltage amplifier. The lateral movement was achieved by dithering the sample in the long axis direction of the cantilever, using the piezo tube with an oscillatory signal of about 1 nm amplitude at the frequency of 100 Hz (Goddenhenrich et al., 1994; Goertz et al., 2007;Major et al., 2006). A Hewlett-Packard function generator (model 33120A) was used to generate the oscillatory signal. The piezo tube sensitivities in the x and y-direction are calibrated to be 6.25nm/V and the sensitivity in the z-direction is 3.65nm/V. The amplitude of the ac-component $V_{ZnO,ac,}$ was measured using a lock-in amplifier (7225 DSP, Signal Recovery, Oak Ridge, TN) with a time constant and sensitivity of 100 ms and voltage gain of 100 mV, respectively. V_{A-B}, $V_{ZnO,dc}$ and the lock-in output $V_{ZnO,ac}$ were recorded using the analog-to-digital converter of the RHK controller system. All data processing and analysis were performed with Kaleidagraph (Synergy Software, Reading, PA) after raw data acquisition.

In the present design, a cantilever with a built-in ZnO stack called a "dimension micro-actuated silicon probe" (DMASP) is employed as the COIFM sensor (DMASP, Bruker Corporation, Santa Barbara, CA). The DMASP cantilever acts as not only a detector, but also an actuator due to the ZnO stack. Voltage-activated mechanical bending of the ZnO stack serves for the force feedback in response to a displacement detection signal. The ZnO feedback loop is capable of feeding back high-frequency signals (or small forces) due to the wide frequency response of up to ~50 kHz, which is a hundred times larger than the z-bandwidth of the piezo tube feedback loop of the ordinary AFM. Thus, the feedback loop allows for more rapid, precise and accurate force measurements than ordinary commercial AFM systems in the force-distance curve. Instead of applying an opposing force on the force sensor through force-feedback, as is the case of the existing IFM, the COIFM attains zero compliance by relieving the strain built on the cantilever. This feedback mechanism protects the tip from being damaged in conjunction with the flexible spring of DMASP, thus allowing repeated use of the force sensor and improving reliability of the measurement.

Figure 1(b) shows the DMASP cantilever with the inset showing a close up of the tip. This probe is made of 1-10 Ωcm Phosphorus doped Si, with a nominal spring constant (k_z) and resonance frequency known to be 3 N/m and 50 kHz, respectively (Bruker Corp., 2011). The dimensions were measured to be L_{cant} = 485 μm, L_{tip} = 20 μm, which is in agreement with other previous measurements (Rogers et al., 2004; Vázquez et al., 2009). L_{cant} is the length of the portion of the cantilever between the base of the cantilever and the tip. A nanometer diameter tip underneath the cantilever allows for measuring the intermolecular interaction at the single molecular level between the tip and a surface. The cantilever has zero compliance during the measurement, thus preventing the snap-to-contact process associated with typical AFM force-distance measurements. Additionally, the sharp tip of the DMASP leads to probing the local structure of the interfacial water without averaging out the interfacial forces between the tip and the surface.

3. Theoretical background of COIFM with lateral modulation

3.1 Coupling of normal and friction forces through cantilever displacement

The cantilever-based optical interfacial force microscope is a combination of the AFM and IFM. The integrated COIFM employs an optical detection method of AFM and a micro-

actuated silicon cantilever to self-balance the force sensor, which improves the interfacial force sensitivity by an order of magnitude and the spatial sensitivity to the sub-nanometer scale. This is enough to resolve molecular structures, such as the individual water ordering.

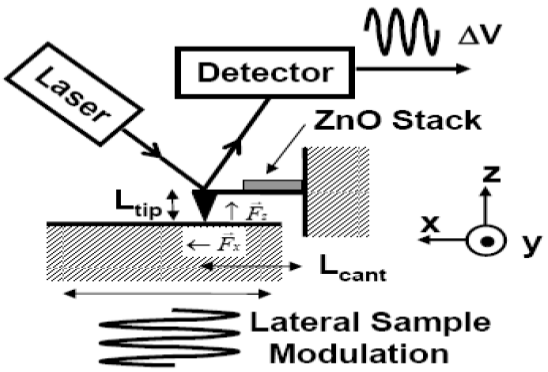

Fig. 2. The optical detection scheme of the AFM using a DMASP tip, including the applied modulation and forces. **(**Reprinted with permission from Rev. Sci. Instrum. **82,** 053711 (2011). Copyright 2011 American Institute of Physics.)

Figure 2 illustrates an optical beam displacement detection scheme in the AFM head that was used to transmit the interaction forces between the tip and the surface into an electrical signal (E. Meyer et al., 1988). The tip of the cantilever experiences the forces $F_{x \text{ and }} F_z$ by the sample surface during force measurements. A general Euler equation (Thomson, 1996) is given for the vertical displacement of the cantilever (z_z) produced by the normal force (F_z) acting at a point x = L_{cant} as follows (Chen, 1993; Sarid, 1991),

$$F_z(L_{cant} - x) = EI\frac{d^2 z_z}{dx^2} \tag{1}$$

where L_{cant} is the length of the cantilever, E is the Young's Modulus and z_z is the vertical displacement caused by F_z. The area moment of inertia (I) for a rectangular bar is given by,

$$I = \frac{t^3 w}{12} \tag{2}$$

where t is the bar thickness, and w is the width of the bar. The solution to the above equation with the boundary condition $z_z\big|_{z=0} = 0$, $\left.\frac{dz_z}{dx}\right|_{z=0} = 0$, is as follows,

$$z_z = \frac{3F_z}{2k_z}(\frac{x}{L_{cant}})^2(1 - \frac{x}{3L_{cant}}) \tag{3}$$

where the spring constant (k_z) is defined as the following (Sader, 2003; Sader & Green, 2004; Neumeister, 1994).

$$k_z = \frac{Et^3 w}{4L_{cant}^3} \tag{4}$$

In addition to the vertical force F_z, a friction force (F_x) along the major axis of the cantilever (see **Figure 2**) also contributes to the vertical displacement of the cantilever by the following Euler equation:

$$F_x L_{tip} = EI \frac{d^2 z_x}{dx^2} \tag{5}$$

where L_{tip} is the length of the cantilever tip. The vertical displacement produced by F_x(z_x) can then be found in the following equation:

$$z_x = \frac{3F_x}{2k_z} \cdot \frac{L_{tip}}{L_{cant}} (\frac{x}{L_{cant}})^2 \tag{6}$$

The total displacement (z_c), the sum of both $z_z$and z_x, is given by the following equation:

$$z_c = \frac{3}{2k_z} (\frac{x}{L_{cant}})^2 \left[\frac{L_{tip}}{L_{cant}} F_x + (1 - \frac{x}{3L_{cant}}) F_z \right] \tag{7}$$

The bending motion of the cantilever due to the tip-sample interactions is detected by measuring the voltage difference ($V_{A\text{-}B}$) between two photodiodes, namely A and B, as shown in **Figure 1(a)**. The difference in voltage is proportional to the slope of the cantilever (according to the law of reflection) at the point (x=L_{cant}) where the beam is reflected as follows (Schwarz et al., 1996):

$$V_{A-B} = \alpha \vartheta_c \tag{8}$$

where α is a proportional constant. The total slope (ϑ_c) at x=L_{cant} is the derivative of total displacement of the cantilever (as given in equation (7)) with respect to z in the following way:

$$\vartheta_c = \left. \frac{dz_c}{dx} \right|_{x=L_{cant}} = \frac{3}{2k_z L_{cant}} \left(F_z + 2 \frac{L_{tip}}{L_{cant}} F_x \right) \tag{9}$$

The above relation is consistent with an earlier work (Sader, 2003). The detection signal $V_{A\text{-}B}$ is related to the two forces as follows:

$$V_{A-B} = \frac{3\alpha}{2k_z L_{cant}} (F_z + \frac{2L_{tip}}{L_{cant}} F_x) \tag{10}$$

The above relation enables one to measure the normal force F_z and the friction force F_x simultaneously through the measurement of the optical beam displacement signal, $V_{A\text{-}B}$.

However, the inability of the current AFM system to control the cantilever displacement causes limitations in measuring forces using equation (10) over all distance ranges due to the snap-to-contact problem.

3.2 Voltage activated force feedback

We apply the concept of the COIFM technique to the simultaneous measurement of normal and friction forces on approach to overcome the limitations of the AFM, using the DMASP cantilever as a detector and an actuator. Here we apply this concept to the case where friction force (F_x) and normal force (F_z) exist together by making displacement zero while measuring the normal force F_z through the voltage activated force feedback (Bonander & B.I. Kim, 2008). When in feedback, the detector signal ($V_{A\text{-}B}$) in **Figure 1(a)** is maintained at zero by generating a feedback force $F_{feedback}$ as follows:

$$V_{A-B}(t) = \frac{3\alpha}{2k_z L_{cant}} \left(F_z + 2\frac{L_{tip}}{L_{cant}} F_x - F_{feedback} \right) = 0 \tag{11}$$

In the voltage activated force feedback, a voltage V_{ZnO} is applied to the ZnO stack of the DMASP cantilever. Because V_{ZnO} is linearly proportional to $V_{A\text{-}B}$ with a proportional constant β as given,

$$V_{A-B} = \beta \cdot V_{ZnO} \tag{12}$$

the feedback condition in equation (11) can be solved in terms of V_{ZnO} as follows:

$$V_{ZnO} = \frac{3\alpha}{2\beta k_z L_{cant}} \left(F_z + \frac{2L_{tip}}{L_{cant}} F_x \right) \tag{13}$$

This equation suggests that the ability to obtain normal and friction forces while overcoming the snap-to-contact problem will make feedback measurements much more advantageous than non-feedback measurements. Equation (13) suggests that instead of the $V_{A\text{-}B}$ signal, the feedback signal V_{ZnO} is used in measuring normal and friction forces.

4. Calibration of COIFM

4.1 Feedback response test

To find the time resolution of the COIFM, a square-wave voltage with amplitude 0.2 V and frequency 10 Hz was applied to the set-point voltage ($V_{set\ point}$) with the force feedback far away from the surface (B.I. Kim, 2004). **Figure 3(a)-3(d)** shows that the feedback controller preamp output ($V_{A\text{-}B}$) follows this square wave by applying appropriate voltages to the ZnO stack of the DMASP sensor (V_{ZnO}). The square wave causes the cantilever to try to create a torque on the cantilever so as to achieve a zero error voltage V_{Error} with the feedback on (**Figure 3(c)**). The controller is set up to optimize the transient response in order to achieve the necessary time response for a COIFM experiment. The transient feedback response test signal (**Figure 3(d)**) shows that the COIFM has a practical time resolution ~ 1.5 msec. The force resolution is less than 150 pN, which is a higher force sensitivity by two orders of magnitude than the existing IFM with electrical detection method (Joyce & Houston, 1991).

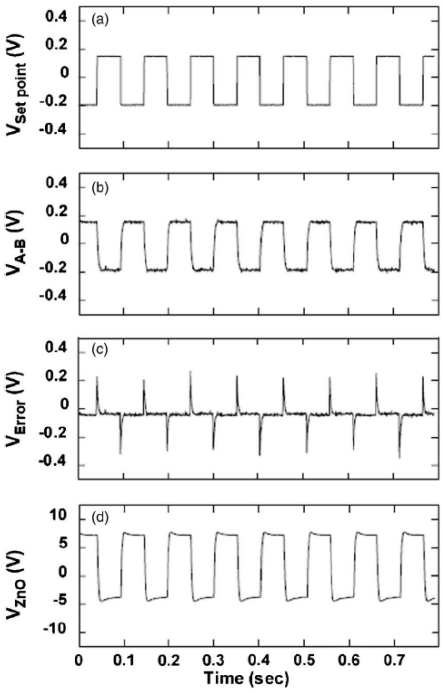

Fig. 3. **(a)** A square wave ac signal with a frequency of 10 Hz as a set-point voltage of the feedback loop. **(b)** The deflection V_{A-B} signal that follows the set-point voltage. **(c)** The error signal V_{Error}between $V_{Set-point}$ and $V_{A-B.}$ **(d)** The signal V_{ZnO} sent from the controller to the ZnO stack material. (Reprinted with permission from Appl. Phys. Lett. **92**, 103124 (2008). Copyright 2008 American Institute of Physics.)

4.2 Normal and friction force calibration

A lock-in amplifier (7225 DSP, Signal Recovery, Oak Ridge, TN) is used to generate a sinusoidal driving signal and to detect the modulated output of the force sensor. By dithering the tip in the x-axis with amplitude 3 nm at 100 Hz and detecting the response amplitude with a lock-in amplifier, we can measure normal force and friction force simultaneously as a function of separation distance. With an amplitude of 100 mV at a load force of 10-20 nN, the friction force is typically 3-6 nN.

For qualitative understanding, the signal V_{A-B} should be converted into force using the relation between the signal and the two forces in equation (10). Equation (10) suggests how to calibrate the conversion factors from the V_{A-B} signal to both forces experimentally. To do this we need to find the proportional constant α between V_{A-B} and ϑ_c. When the tip is in contact with the substrate, the detection signal can be expressed as:

$$V_{A-B} = \frac{3\alpha}{2L_{cant}} z_c \tag{14}$$

where z_c is the cantilever displacement along z-axis. The above equation suggests that α can be found by measuring the V_{A-B} signal as a function of z_c. The cantilever displacement can be changed systematically by contacting the cantilever to the sample surface (assuming that the indentation between the tip and the surface is negligible).

If an external friction force is applied to the probe tip, the system will be balanced by generating an additional force by a change in voltage. The output is the force feedback voltage to maintain zero compliance in the cantilever and represents the interfacial friction force between tip and sample. The actual force applied to the tip is related to the voltage sent to the ZnO stack via "voltage-to-force conversion factor." In actual operation, the controller system records variations in the voltage applied to the ZnO stack as a function of relative tip/sample separation. To experimentally determine the value of the voltage-to-force conversion factor, two measurements are taken. The first measurement is done with the tip in contact with the substrate. As a voltage is applied to the piezo tube, the piezo tube moves, causing the cantilever to bend. The optical beam detection will record a change in voltage. A plot is made of the change in detection signal versus distance, and the slope of the line $\left(\frac{3\alpha}{2L_{cant}}\right)$ is found to be 20.4 mV/nm from the relationship between V_{A-B} and z_c shown in **Figure 4(a)**. From the figure, α is found to be 6.60×10^3 V/rad with L_{cant} = 485μm. The normal force conversion factor from V_{A-B} into F_z is determined to be 147 nN/V from $\frac{2k_z L_{cant}}{3\alpha}$ with the spring constant k_z of ~3 N/m.

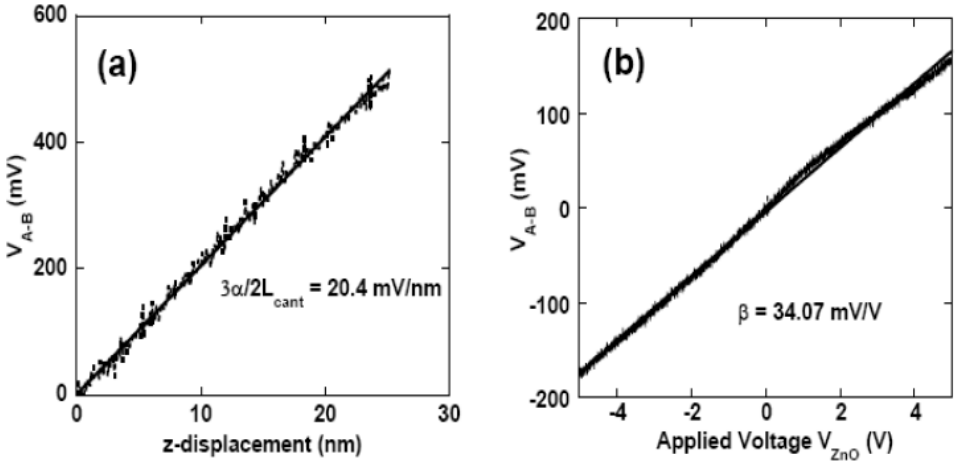

Fig. 4. **(a)** Change in V_{A-B} versus cantilever displacement (z_c) due to normal force. The slope of the line allows us to determine the conversion factor α. **(b)** The resulting change in V_{A-B} when a voltage is applied to the ZnO stack from -10 V to 10 V. The slope of this line is β and is used in the equation to find the voltage-to-force conversion factor. (Reprinted with permission from Rev. Sci. Instrum. **82**, 053711 (2011). Copyright 2011 American Institute of Physics.)

The second measurement is done with the tip not in contact with the substrate. Here a voltage is applied to the cantilever, causing it to bend. Again, the change in voltage of the optical beam detection method is recorded (see Figure 4(b)). The slope of the line is the constant β which is found to be 34.07 mV/V through the linear fitting of the data in **Figure 4(b)**. Using the obtained α value along with the measured β value, and the spring constant, the calculated conversion factor for normal forces while the system is in feedback $\left(\frac{2\beta k_z L_{cant}}{3\alpha}\right)$ is found to be 5.01 nN/V. Using L_{tip} = 20 μm (Bruker Corp., 2011), the conversion factor for friction forces $\frac{\beta k_z L_{cant}^2}{3\alpha L_{tip}}$ is calculated to be 182.14 nN/V. It is important to note that this lateral conversion factor is 12 times larger than the normal force conversion factor because of $\frac{L_{cant}}{2L_{tip}}$ in equation (13).

5. Demonstration of COIFM in measuring force-distance curves

The capability of this COIFM as a second generation of IFM has been demonstrated by revealing the hidden structures of the interfacial water on a silicon surface at the molecular scale. **Figure 5(a)** illustrates a typical force distance curve taken on a silicon surface (SPI Supplies) in air with feedback off as the tip approaches with the speed of 8 nm/s at a distance of 50 nm away from the surface. In the force-displacement curve, the distance zero was defined as the intersection between the contact force line and the line where the interfacial force is zero (Senden, 2001). The voltage units were converted into force units using the conversion factors found above, as shown on the right axis of each panel. A long-range repulsive force appears monotonously at the distances between 5 nm and 30 nm from the silicon surface, possibly resulting from the electrostatic dipole-dipole interaction observed by Kelvin probe measurement (Verdaguer et al., 2006). The same experiment was repeated with the feedback ON. The voltage signal to the ZnO material, V_{ZnO}, and the error signal $V_{A\text{-}B}$ were recorded as a function of tip to sample distance, as shown in **Figure 5(b)** and **Figure 5(c)**, respectively. One of the key features in **Figure 5(c)** is that the $V_{A\text{-}B}$ voltage remains zero during approach, indicating that all forces on the cantilever remain balanced or "zero compliance" by relieving the strain built up in the ZnO stack through force feedback. However, the sensing cantilever starts to bend as soon as the tip touches the silicon surface, indicating the breakdown of force feedback. The long- range interaction is reproducibly obtained in the force-distance curve with feedback on (**Figure 5(b)**). The background noise level (0.1~0.2 nN) is smaller than the background noise (1~2 nN) with feedback off by an order of magnitude.

Direct comparison between two force curves with feedback on and off in the distance range between 0 nm and 5 nm shows that fine periodic structures with several peaks and valleys appear from the surface in the force curve with feedback on, whereas they are not absent in the force-displacement curve with feedback off. Interestingly, the periodicity of the peaks is 0.32 ± 0.13 nm as marked with arrows in the detailed force-distance curve between 0 nm and 3 nm (inset of **Figure 5(b)**), which is comparable with the diameter of a single water molecule. In recent years, a few groups have observed similar periodic features at interfaces between solid surfaces and liquid water using amplitude modulation methods,

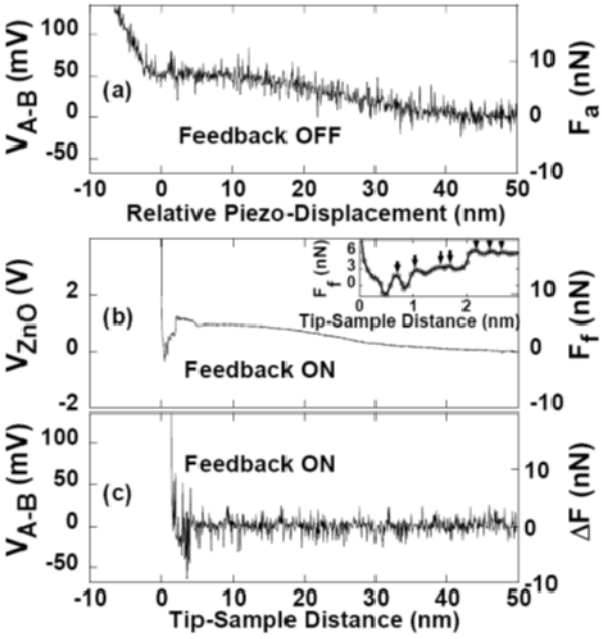

Fig. 5. **(a)** A force-displacement curve between the tip and the silicon surface obtained without a force-activated voltage feedback system. **(b)** The force applied to the ZnO stack material was graphed as a function of tip and silicon sample distance. **(c)** Force-distance curve between the tip and the silicon surface obtained with a force-activated voltage feedback system. (Reprinted with permission from Appl. Phys. Lett. **92**, 103124 (2008). Copyright 2008 American Institute of Physics.)

suggesting the possible ordering of water molecules near surfaces (Antognozzi et al., 2001; Jarvis et al., 2000; Jeffery et al., 2004; Uchihashi et al., 2005). This COIFM data on interfacial water demonstrates that the COIFM is capable of unveiling structural and mechanical information on interfacial water at the single molecular level, which has not been previously reported with the existing IFM. In contrast to the recent IFM studies of interfacial water, in which IFMs large diameter (1 μm-10 μm) tips were used (Major et al., 2006; Matthew et al., 2007), the sharp tip of the DMASP was able to probe the local structure of the interfacial water without averaging out the interfacial forces between the tip and the surface.

6. Application of COIFM to moleular interaction measurements

6.1 Background

The capability of the COIFM over both the IFM and AFM systems is demonstrated by measuring friction forces and normal forces generated by the water molecules in an ambient environment. Friction is of great importance in micromechanical systems where water is trapped between two surfaces (Komvopoulos, 2003). The trapped water has a critical effect on the performance of the systems through interfacial tribological properties (de Boer &

Mayer, 2001). This could include the roles of water in inter-molecular/inter-surface friction and in the reduction of the friction in water-based bio-materials such as artificial cartilage. Water molecules in bulk water are understood as being ordered at the liquid-solid interface, with that order decaying with each water molecule's distance from the interface (Jarvis et al., 2000).

Far less is known, comparatively, about the structure of interfacial water in ambient conditions (Verdaguer et al., 2006). In an ambient environment, in addition to interacting with the substrate surface, the interfacial water also interacts with the surrounding water vapor. More recent attempts have been made to describe the viscosity of interfacial water using the IFM (Goertz, 2007; Major et al., 2006). The structured water exists not only on crystalline hydrophilic surfaces, but even on amorphous surfaces (Asay & S.H.J. Kim, 2005, 2006; Verdaguer et al., 2006). These studies indicate that the behavior of interfacial water molecules in an ambient environment is substantially different from the behavior of water at the liquid-solid interface. Here we applied the developed COIFM to probe the structure of interfacial water.

6.2 Materials and methods

All measurements were taken on a freshly cleaned silica wafer, Si (100) (SPI Supplies, West Chester, PA), in an ambient condition with the relative humidity monitored using a thermo-hygro recorder (Control Co., Friendswood, TX). The top of the surface is expected to be covered with natural oxide in air, thereby forming the silica, the most abundant material in the Earth's crust (Iler, 1979). The wafer was attached to a 15 mm steel disk using double-stick tape and then mounted on a magnetic sample stage on top of the piezo tube. To remove all organic contaminates, the silica was cleaned using a piranha solution made from a 3:1 concentrated H_2SO_4/30% H_2O_2 (Pharmco and Fischer Scientific, respectively). It was then sonicated in acetone for 5 minutes, then in ethanol for 5 minutes, rinsed with DI water, and then dried with a dry N_2 flow. Tips were cleaned using a UV sterilizer (Bioforce Nanosciences Inc., Ames, IA) to remove the residual hydrocarbon molecules. The tip speed was chosen as 10 nm/sec. The output signals of the lock-in amplifier were converted into forces using the conversion factors found in the results section. The converted force scales are displayed on the right axis of each panel and voltage units on the left axis.

6.3 Large oscillatory force of water in an ambient condition

We also measured both normal and friction forces in the water junction between the probe and the surface with the COIFM with lateral modulation. **Figure 6(a), 6(b)** and **6(c)** show the measured $V_{A\text{-}B}$, $V_{ZnO,ac}$, and $V_{ZnO,dc}$ data, respectively, as a function of piezo displacement. The data clearly demonstrates that the force feedback allows for the COIFM to measure the normal force of water between the tip and the sample for all distance regimes, overcoming the snap-to-contact effect associated with the conventional AFM method. The zero distance was defined as the point where the friction force increases sharply as marked in **Figure 6(b)**. As the tip approaches, both normal and friction forces remain at zero until interaction with interfacial water occurs around 12 nm away from the substrate. Surprisingly, the data show oscillatory patterns in both normal force and friction force. The $V_{A\text{-}B}$ signal also displays a periodic change with the tip-sample distance, as shown in an enlarged inset in **Figure 6(a).** These periodic features are consistent with the earlier AFM-based observation of a stepwise

change of the force gradient related with the thin water bridge in an ambient environment (Choe et al., 2005). The absence of modulation turns out to decrease the number of oscillations by several times, therefore suggesting that the kinetic energy due to the lateral modulation promotes layering transitions by overcoming the activation barriers between two successive layered states of the interfacial water.

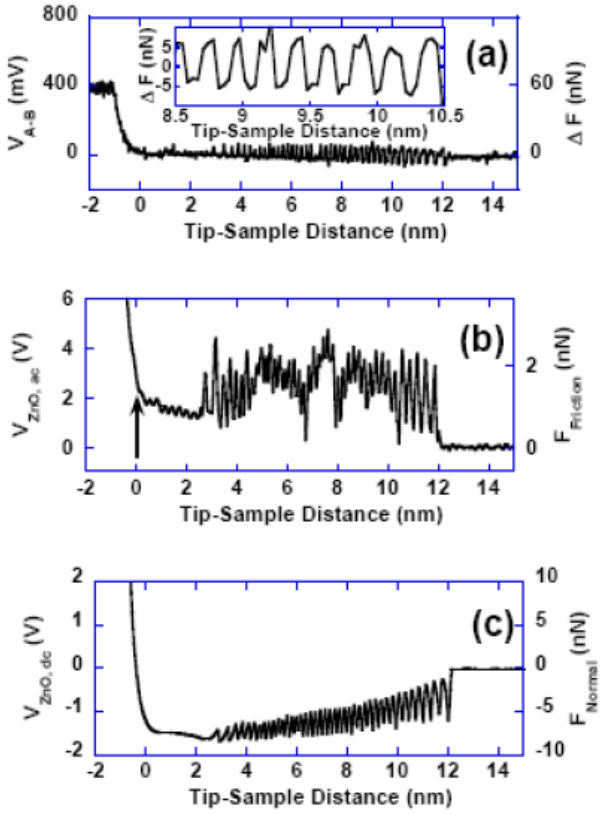

Fig. 6. Force-distance curves for $V_{A\text{-}B}$ **(a)**, the frictional force **(b)**, and normal force **(c)** during the tip-approach towards the surface with velocities of 10 nm/s at 55% relative humidity. The inset in **(a)** is an expanded plot of $V_{A\text{-}B}$ in a range of 8.5 - 10.5 nm. (Reprinted with permission from Rev. Sci. Instrum. **82**, 053711 (2011). Copyright 2011 American Institute of Physics.)

The periodicity is found to be 0.227±0.056 nm for valley-valley distance analysis and 0.223±0.055 nm for peak-peak distance analysis. This periodicity matches the diameter of water, which is consistent with Antognozzi et al., who found the periodicity of water layers to be 0.24-0.29 nm even for distilled water deposited on a mica sample surface using a near-field scanning optical microscope (NSOM) (Antognozzi et al., 2001). This result is also in agreement with other earlier studies using AFM at the liquid-solid interface between a hydrophilic surface (e.g., mica) and bulk water (Higgins et al., 2006; Jarvis et al., 2000; Jarvis

et al., 2001; Jeffery et al., 2004; Li et al., 2007; Uchihashi et al., 2005). The interfacial water confined between two surfaces forms water layers with periodicity of one water diameter 0.22 nm (Jarvis et al., 2000), 0.23 +0.003 nm (Jarvis et al., 2001), 0.25 + 0.05 nm (Jeffery et al., 2004), 0.23 ± 0.03 nm (Uchihashi et al., 2005), 0.29 ± 0.006 nm (Higgins et al., 2006), and 0.22-0.29 nm (Li et al., 2007). This can be understood that the ordering of confined water molecules leads to oscillatory solvation forces, which are reflections of the geometric packing experienced by the molecules due to the imposing surfaces, with the period of oscillation roughly equal to the molecular diameter of water. The oscillations occur in the molecular force due to the transition between solid (ordering) and liquid (disordering), depending on the commensuration and incommensuration between the spacing and the molecular diameter (Chaikin & Lubensky, 1995). These data on the interfacial water suggest that the COIFM is capable of providing unprecedented information on the structural and mechanical properties of molecules.

Most published data concerning interfacial water has never shown distinct oscillatory behavior (Goertz, 2007; Major et al., 2006). This is because previous methods exhibit too much noise to see the distinct oscillatory patterns or have mechanical instabilities that prevent measurements over all distance regimes. One important aspect of data collection that is visible in **Figure 6** is the lack of noise in COIFM data. This lack of noise is due to the size of the tip and the sensitivity of the system. With the lack of noise, a very distinct oscillatory pattern can be seen in both normal and friction force, which starts with onset of chain formation and continues until the tip and sample come in contact. Also, due to the lack of noise, it is evident that a peak in normal force corresponds to a peak in friction force. Once the tip and sample come in contact, there is a very sharp rise in normal force and an increase in friction force as well. So the amount of noise in IFM data makes it difficult to see the correlation that is present in COIFM data. The COIFM employs an optical detection method of AFM and a commercially available micro-actuated silicon cantilever to self-balance the force sensor, which improves the interfacial force sensitivity by an order of magnitude and the spatial sensitivity to the sub-nanometer scale, enough to resolve the individual water ordering on a silicon surface. The change in tip size and increased sensitivity for electric force detection in the COIFM in comparison to the IFM allows it to be used at the sub-nanometer range and make it a more useful technique in analyzing forces at nanoscopic ranges. While simultaneous measurement of normal and friction forces is not new, the resolution with which they have been measured by the COIFM is novel.

7. Conclusion

Here we reported the integration of the existing two scanning-probe techniques (AFM and IFM) through the development of an instrument called a "cantilever-based optical interfacial force microscope" (COIFM) (Bonander & B.I. Kim, 2008). The COIFM is a new tool developed for the study of interfacial forces, such as interfacial water structural forces. The COIFM employs a commercially available "dimension micro-actuated silicon probe" (DMASP) cantilever in its voltage-activated force feedback scheme (Aimé et al., 1994; Burnham & Colton, 1989; Lodge, 1983; G. Meyer & Amer., 1988). The diminished size of the DMASP cantilver at a radius of 10 nm, compared to that of the IFM's 0.1 μm to 1 μm probe radius, enables one to study water structures at the single molecular level. The smaller probe size of the cantilever enables improved force resolution over conventional techniques

by at least an order of magnitude. Additionally, due to the optical detection scheme, the force resolution is improved by two orders of magnitude over the existing IFM with electrical detection method (Joyce & Houston, 1991). The ZnO feedback loop allows for more rapid, precise and accurate force measurements than ordinary commercial AFM systems in the force-distance curve. The COIFM attains zero compliance by relieving the strain built on the cantilever protecting the tip from being damaged in conjunction with the flexible spring of DMASP, thus allowing repeated use of the force sensor and improving reliability of the measurement.

The recently developed COIFM technique was used to measure normal and friction forces simultaneously for studies of interfacial structures and mechanical properties of nanoscale materials. We derived how the forces can be incorporated into the detection signal using the classical Euler equation for beams. A lateral modulation with the amplitude of one nanometer was applied to create the friction forces between tip and sample. The COIFM with lateral modulation allows for simultaneous measurement of normal and friction forces in the attractive regime as well as in the repulsive regime by utilizing the force feedback capability of the instrument (Bonander & B.I. Kim, 2008). We demonstrated the capability of the COIFM by measuring normal and friction forces of interfacial water at the molecular scale over all distance ranges. It also demonstrated the capability of this COIFM as a second generation of the IFM by revealing the hidden structures of the interfacial water between two silica surfaces (Bonander & B.I. Kim, 2008). The distinct oscillations observed when measuring interfacial water potentially will reveal new information about molecular water orientation with further analysis of the data. Although there have been many friction measurements using scanning probe techniques, there are few explicit relations between the detection signal, normal, and frictional forces. The ability of COIFM to measure normal and friction force simultaneously, along with the incorporation of force-feedback control, make this type of microscopy a very useful technique in analyzing thin films and interactions between two surfaces, especially when measuring large amounts of force are necessary.

8. Future applications

Due to its excellent capability, the COIFM will improve the understanding of hidden interfacial phenomena. The COIFM will reveal new information about interfacial water and also other molecules where conventional AFM and IFM systems have been used, such as DNA (Hansma et al., 1996). The usefulness and uniqueness of the COIFM in studying unprecedented structural and mechanical properties of interfacial water confined between a tip and a sample surface has already been characterized. Future applications of the COIFM will be extended to the recognition and investigation of biomolecular interactions.

Intermolecular friction forces play a fundamental role in many biological processes, such as transport along cytoskeletal filaments (Mueller et al., 2010) or inside human and animal joints (Flannery et al., 2010). Biomolecular functions are the most important phenomena to sustain our lives (Alberts, 2002). They carry out delicate structural conformation changes along the reaction coordinates during the biomolecular activation. The conformation changes are related to metastable intermediate states and energy barriers due to chemical and mechanical forces between a protein and a protein, between a protein and a ligand, and within proteins (Schramm, 2005). Correlating the metastable intermediate states and energy barriers with known structural information is extremely important in understanding each

step of the biomolecular functions. A biomolecular system passes through several metastable states before it reaches a stable state with the lowest energy. Even with such importance, however, metastable intermediate states and energy barriers are difficult to observe because of a relatively short life span (~10^{-13} sec) and their non-equilibrium nature in a solution phase (Schramm, 2005). It is for this reason that these extremely important and challenging problems mentioned above remain largely unsolved. As an attempt to solve these problems, instead of controlling the binding time along a reaction coordinate (e.g., using kinetic isotope effects), detaching two bounded single molecules from each other by pulling both ends has been employed as an alternative method (Evans & Ritchie, 1997). The single molecular pulling measurements provide individual molecular value for a physical quantity (e.g., force) under non-equilibrium conditions because the measurement is conducted for each single molecule individually (Evans & Ritchie, 1997; Hermanson, 1995; Lee et al., 1994; Liphardt et al., 2002; Oberhauser et al., 1998; Rief et al., 1997; Ros et al., 1998; Strunz et al., 1999); whereas, the current biomolecular and biochemistry investigations measure the average value of a biochemical quantity over a huge number of molecules (~ 10^{23}) under equilibrium conditions. The COIFM's sensitive distance and force control capability allows for investigating the metastable states along the reaction coordinates level.

9. Acknowledgment

The author thanks Jeremy Bonander, Jared Rasmussen, Ryan Boehm, Edward Kim, Joseph Holmes, and Thanh Tran for all their help and support on this project. This work is partly funded by NSF DMR-1126854, NSF DBI-0852886, NSF EPSCOR Startup Augmentation Funding, and the Research Corporation Single-Investigator (Cottrell College Science Award No. CC7041/7162).

10. References

Aimé, J.P., Elkaakour, Z., Odin, C., Bouhacina, T., Michel, D., Curély, J., & Dautant, A. (1994). Comments on the use of the force mode in atomic force microscopy for polymer films. *J. Appl. Phys.*, Vol. 76, No. 2, (July 1994), pp. (754-762), 0021-8979

Alberts, B. (2002). *Molecular biology of the cell* **(**4th Ed.)**,** Garland Science, 978-0815332183, New York

Antognozzi, M., Humphris, A.D.L., & Miles, M.J. (2001). Observation of molecular layering in a confined water film and study of the layers viscoelastic properties. *Appl. Phys. Lett.*, Vol. 78, No. 3, (January 2001), pp. (300-302), 0003-6951

Asay, D.B., & Kim, S.H. (2005). Evolution of the adsorbed water layer structure on silicon oxide at room temperature. *J. Phys. Chem. B*, Vol. 109, No. 35, (August 2005), pp. (16760-16763), 1520-6106

Asay, D.B., & Kim, S.H. (2006). Effects of adsorbed water layer structure on adhesion force of silicon oxide nanoasperity contact in humid ambient. *J. Chem. Phys.*, Vol. 124, No. 17, (May 2006), pp. (174712/1-174712/5), 0021-9606

Ashby, P.D., Chen, L., & Lieber, C.M. (2000). Probing intermolecular forces and potentials with magnetic feedback chemical force microscopy. *J. Am. Chem. Soc.*, Vol. 122, No. 39, (September 2000), pp. (9467-9472)

Bonander, J.R., & Kim, B.I. (2008). Cantilever based optical interfacial force microscope. *Appl. Phys. Lett.*, Vol. 92, No. 10, (March 2008), pp. (103124), 0003-6951

Bruker Corporation (2011). *Probes and Accessories*, Bruker, Camarillo, CA

Bunker, B.C., Kim, B.I., Houston, J.E., Rosario, R., Garcia, A.A., Hayes, M., Gust, D., & Picraux, S.T. (2003). Direct observation of photo switching in tethered spiropyrans using the interfacial force microscope. *Nano Lett.*, Vol. 3, No. 12, (November 2003), pp. (1723-1727)

Burnham, N.A., & Colton, R.J. (1989). Measuring the nanomechanical properties and surface forces of materials using an atomic force microscope. *Journal of Vacuum Science Technology A: Vacuum, Surfaces, and Films*, Vol. 7, No. 4, (July 1989), pp. (2906 -2913), 0734-2101

Burns, A.R., Houston, J.E., Carpick, R.W., & Michalske, T.A. (1999A). Friction and molecular deformation in the tensile regime. *Phys. Rev. Lett.*, Vol. 82, No. 6, (February 1999), pp. (1181-1184), 0031-9007

Burns, A.R., Houston, J.E., Carpick, R.W., & Michalske, T.A. (1999B). Molecular Level Friction As Revealed with a Novel Scanning Probe. *Langmuir*, Vol. 15, No. 8, (April 1999), pp. (2922-2930)

Butt, H.J., Cappella, B., & Kappl, M. (2005). Force measurements with the atomic force microscope: technique, interpretation and applications. *Surf. Sci. Rep.*, Vol. 59, No. 1-6, (October 2005), pp. (1-152)

Cappella, B., & Dietler, G. (1999). Force-distance curves by atomic force microscopy. *Surface Science Reports*, Vol. 34, No. 1-3, (July 1999), pp. (1-104), 0167-5729

Carpick, R.W., Ogletree, D.F.and Salmeron, M. (1997). Lateral stiffness: a new nanomechanical measurement for the determination of shear strengths with friction force microscopy. *Appl. Phys. Lett.*, Vol. 70, No. 12, (March 1997), pp. (1548-1550), 0003-6951

Chaikin, P.and Lubensky, T. (2000).*Principles of condensed matter physics*, Cambridge University Press, 0-521-43224-3, New York

Chang, K.K., Shie, N.C., Tai, H.M., & Chen, T.L. (2004), A micro force sensor using force-balancing feedback control system and optic-fiber interferometers. *Tamkang Journal of Science and Engineering*, Vol. 7, No. 2, pp. (91-94)

Chen, C. (1993).*Introduction to scanning tunneling microscopy*, Oxford University Press, 0-19-507150-6, New York

Choe, H., Hong, M.H., Seo, Y., Lee, K., Kim, G., Cho, Y., Ihm, J., & Jhe, W. (2005). Formation, manipulation, and elasticity measurement of a nanometric column of water molecules. *Phys. Rev. Lett.*, Vol. 95, No. 18, (October 2005), pp. (187801/1-187801/4), 0031-9007

Colchero, J., Luna, M., & Baró, A.M. (1996). Lock-in technique for measuring friction on a nanometer scale. *Appl. Phys. Lettl.*,Vol. 68, No. 20, (March 1996), pp. (2896-2898), 0003-6951

De Boer, M.P., & Mayer, T.M. (2001). Tribology of MEMS. *MRS Bull.*, Vol.26, No.4, (April 2001) pp. (302-304)

Evans, E. &. Ritchie, K. (1997). Dynamic strength of molecular adhesion bonds, *Biophys. J.*, Vol. 72, No. 4, (April 1997), pp. (1541-1555), 1541-1555

Fernandez-Torres, L., Kim, B.I., & Perry, S. (2003). The frictional response of VC(100) surfaces: influence of 1-octanol and 2,2,2-trifluoroethanol adsorption. *Tribology Letters*, Vol. 15, No. 1, (June 2003), pp. (43-50), 1023-8883

Flannery, M., S. Flanagan, E. Jones and C. Birkinshaw. (2010). Compliant layer knee bearings: part I: friction and lubrication. *Wear*, Vol. 269, No. 5-6, (July 2010), pp. (325-330), 0043-1648

Goertz, M.P., Houston, J.E., & Zhu, X. (2007). Hydrophilicity and the viscosity of interfacial water. *Langmuir*, Vol. 23, No. 10, (May 2007), pp. (5491-5497), 0743-7463

Greenwood, J.A. (1997). Adhesion of elastic spheres. *Proceedings of the Royal Society of London. Series A: Mathematical, Physical and Engineering Sciences*, Vol. 453, No. 1961, (June 1997), pp. (1277-1297), 1471-2946

Göddenhenrich, T., Müller, S., & Heiden, C. (1994). A lateral modulation technique for simultaneous friction and topography measurements with the atomic force microscope. *Rev. Sci. Instrum.*, Vol. 65, No. 9, (September 1994), pp. (2870-2873), 0034-6748

Hansma, H.G., Sinsheimer, R.L., Groppe, J., Bruice, T.C., Elings, V., Gurley, G., Bezanilla, M., Mastrangelo, I.A., Hough, P.V., & Hansma, P.K. (1993). Recent advances in atomic force microscopy of dna. *Scanning*, Vol. 15, No. 5, (Sep-Oct 1993), pp. (296-299), 0161-0457

Hermanson, G.T. (1995). *Bioconjugate techniques* (1st Ed). Academic Press, 978-0123886231, San Diego

Higgins, M.J., Polcik, M., Fukuma, T., Sader, J.E., Nakayama, Y., & Jarvis, S.P. (2006). Structured water layers adjacent to biological membranes. *Biophys. J.*, Vol. 91, No. 7, (October 2006), pp. (2532-2542), 0006-3495

Houston, J.E., & Michalske, T.A. (1992). The interfacial-force microscope. *Nature*, Vol. 356, No. 6366, (March 1992), pp. (266-267), 0028-0836

Huber, D.L., Manginell, R.P., Samara, M.A., Kim, B., & Bunker, B.C. (2003). Programmed adsorption and release of proteins in a microfluidic device. *Science*, Vol. 301, No. 5631, (July 2003), pp. (352-354), 0036-8075

Iler, R.K. (1979).*The chemistry of silica : solubility, polymerization, colloid and surface properties, and biochemistry*, Wiley, New York

Israelachvili, J.N., & Adams, G.E. (1978). Measurement of forces between two mica surfaces in aqueous electrolyte solutions in the range 0-100 nm. *J. Chem. Soc., Faraday Trans. 1*, Vol. 74, No. 0, (January 1978), pp. (975-1001), 0300-9599

Jarvis, S.P., Ishida, T., Uchihashi, T., Nakayama, Y., & Tokumoto, H. (2001). Frequency modulation detection atomic force microscopy in the liquid environment. *Applied Physics A: Materials Science & Processing*, Vol. 72, No. 7, (March 2001), pp. (S129-S132), 0947-8396

Jarvis, S.P., Yamada, H., Yamamoto, S., Tokumoto, H., & Pethica, J.B. (1996). Direct mechanical measurement of interatomic potentials. *Nature*, Vol. 384, No. 6606, (November 1996), pp. (247-249), 1476-4687

Jarvis, S.P., Uchihashi, T., Ishida, T., Tokumoto, H., & Nakayama, Y. (2000). Local solvation shell measurement in water using a carbon nanotube probe. *The Journal of Physical Chemistry B*, Vol. 104, No. 26, (June 2000), pp. (6091-6094), 1520-6106

Jeffery, S., Hoffmann, P.M., Pethica, J.B., Ramanujan, C., Özer, H., & Oral, A. (2004). Direct measurement of molecular stiffness and damping in confined water layers. *Phys. Rev. B*, Vol. 70, No. 5, (August 2004), pp. (054114.1-054114.8), 1098-0121

Joyce, S.A., & Houston, J.E. (1991). A new force sensor incorporating force-feedback control for interfacial force microscopy. *Review of Scientific Instruments*, Vol. 62, No. 3, (March 1991), pp. (710-715), 0034-6748

Kiely, J.D., & Houston, J.E. (1999). Contact hysteresis and friction of alkanethiol self-assembled monolayers on gold. *Langmuir*, Vol. 15, No. 13, (June 1999), pp. (4513-4519), 0743-7463

Kim, B., Lee, S., Guenard, R., Torres, L.F., Perry, S., Frantz, P., & Didziulis, S. (2001). Chemical modification of the interfacial frictional properties of vanadium carbide through ethanol adsorption. *Surface Science*, Vol. 481, No. 1-3, (June 2001), pp. (185 - 197), 0039-6028

Kim, B.I. (2004). Direct comparison between phase locked oscillator and direct resonance oscillator in the noncontact atomic force microscopy under ultrahigh vacuum. *Review of Scientific Instruments*, Vol. 75, No. 11, (November 2004), pp. (5035-5037), 0034-6748

Kim, B.I., Bonander, J.R., & Rasmussen, J.A. (2011). Simultaneous measurement of normal and friction forces using a cantilever-based optical interfacial force microscope. *Review of Scientific Measurements*, Vol. 82, No. 5, (May 2011), pp. (053711), 0034-6748

Kim, H.I., & Houston, J.E. (2000). Separating mechanical and chemical contributions to molecular-level friction. *J. Am. Chem. Soc.*, Vol. 122, No. 48, (August 2000), pp. (12045-12046)

Komvopoulos, K. (2003). Adhesion and friction forces in microelectromechanical systems: mechanisms, measurement, surface modification techniques, and adhesion theory. *Journal of Adhesion Science and Technology*, Vol. 17, No. 4, (May 2003), pp. (477-517)

Lee, G.U., Kidwell, D.A., Colton, R. J. (1994). Sensing discrete streptavidin biotin interactions with atomic-force microscopy. *Langmuir*, Vol. 10, (February 1994), pp. (354-357)

Li, T., Gao, J., Szoszkiewicz, R., Landman, U., & Riedo, E. (2007). Structured and viscous water in subnanometer gaps. *Phys. Rev. B*, Vol. 75, No. 11, (March 2007), pp. (115415/1-115415/6), 1098-0121

Liphardt, J., Dumont, S., Smith, S.B., Tinoco, I., & Bustamante, C. (2002). Equilibrium information from nonequilibrium measurements in an experimental test of jarzynski's equality. *Science*, Vol. 296, No. 5574, (June 2002), pp. (1832-1835)

Lodge, K.B. (1983). Techniques for the measurement of forces between solids. *Advances in Colloid and Interface Science*, Vol. 19, No. 1-2, (July 1983), pp. (27 - 73), 0001-8686

Major, R., Houston, J., McGrath, M., Siepmann, J., & Zhu, X.Y. (2006). Viscous water meniscus under nanoconfinement. *Phys. Rev. Lett.*, Vol. 96, No. 17, (May 2006), pp. (5-8), 0031-9007

Meyer, E., Heinzelmann, H., Grütter, P., Jung, T., Weisskopf, T., Hidber, H., Lapka, R., Rudin, H., & Güntherodt, H. (1988). Comparative study of lithium fluoride and graphite by atomic force microscopy (afm). *Journal of Microscopy*, Vol. 152, No. 1, (October 1988), pp. (269-280), 1365-2818

Meyer, G., & Amer, N.M. (1988). Novel optical approach to atomic force microscopy. *Appl. Physics. Lett.*, Vol. 53, No. 12, (September 1988), pp. (1045-1047), 0003-6951

Müller, M.J., Klumpp, S., & Lipowsky, R. (2010). Bidirectional transport by molecular motors: enhanced processivity and response to external forces. *Biophys. J.*, Vol. 98, No. 11, (June 2010), pp. (2610 - 2618), 0006-3495

Neumeister, J.M., & Ducker, W.A. (1994). Lateral, normal, and longitudinal spring constants of atomic force microscopy cantilevers. *Review of Scientific Instruments*, Vol. 65, No. 8, (August 1994), pp. (2527-2531), 0034-6748

Noy, A., Vezenov, D.V., & Lieber, C.M. (1997). Chemical force microscopy. *Annual Review of Materials Science*, Vol. 27, No. 1, (August 1997), pp. (381-421), 0084-6600

Oberhauser, A.F., Marszalek, P.E., Erickson, H.P., & Fernandez, J.m., (1998). The molecular elasticity of the extracellular matrix protein tenascin. *Nature*, Vol. 393, (February 1998), pp. (181-185), 0028-0836

Rief, M., Gautel, M., Oesterhelt, F., Fernandez, J.M., & Gaub, H.E., (1997). Reversible unfolding of individual titin immunoglobulin domains by AFM. *Science*, Vol. 276, No. 5315, (May 1997), pp. (1109-1112)

Rogers, B., Manning, L., Sulchek, T., & Adams, J. (2004). Improving tapping mode atomic force microscopy with piezoelectric cantilevers. *Ultramicroscopy*, Vol. 100, No. 3-4, (August 2004), pp. (267 - 276), 0304-3991

Ros, R. Schwesinger, F., Anselmetti, D., Kubon, M., Schafer, R., Pluckthun, A., & Tiefenauer, L. (1998) Antigen binding forces of individually addressed single-chain Fv antibody molecules. *Proc. Natl. Acad. Sci. USA,* Vol. 95, No. 13, (June 1998), pp. (7402-7405)

Sader, J.E., & Green, C.P. (2004). In-plane deformation of cantilever plates with applications to lateral force microscopy. *Rev. Sci. Instrum.*, Vol. 75, No. 4, (April 2004), pp. (878-883), 0034-6748

Sader, J.E. (2003). Susceptibility of atomic force microscope cantilevers to lateral forces. *Rev. Sci. Instrum.*, Vol. 74, No. 4, (April 2003), pp. (2438-2443), 0034-6748

Sarid, D. (1994).*Scanning force microscopy: with applications to electric, magnetic, and atomic forces*, Oxford University Press, 0-19-509204-X, Oxford University, New York

Schramm, V.L. (2005) Enzymatic Transition States: Thermodynamics, dynamics and analogue design. *Arch. Biochem. Biophys.,* Vol. 433, No. 1, (January 2005), pp. (13-26), 0003-9861

Schumakovitch, I., Grange, W., Strunz, T., Bertoncini, P., Güntherodt, H., & Hegner, M. (2002). Temperature dependence of unbinding forces between complementary dna strands. *Biophys. J.*, Vol. 82, No. 1, (January 2002), pp. (517-521), 0006-3495

Schwarz, U.D., Köster, P., & Wiesendanger, R. (1996). Quantitative analysis of lateral force microscopy experiments. *Rev. Sci. Instrum.*, Vol. 67, No. 7, (July 1996), pp. (2560-2567), 0034-6748

Senden, T.J. (2001). Force microscopy and surface interactions. *Current Opinion in Colloid & Interface Science*, Vol. 6, No. 2, (May 2001), pp. (95 - 101), 1359-0294

Stewart, A.M., & Parker, J.L. (1992). Force feedback surface force apparatus: principles of operation. *Rev. Sci. Instrum.*, Vol. 63, No. 12, (December 1992), pp. (5626-5633), 0034-6748

Strunz, T., Oroszlan, K., Schafer, R., & Guntherodt, H.J. (1999). Dynamic force spectroscopy of single DNA molcules. *Proc. Natl. Acad. Sci. USA*, Vol. 96, (September 1999) pp. (11277-11282)

Thomson, W. (1993). *Theory of vibration with applications* (4th edition), Prentice-Hall, New York

Uchihashi, T., Higgins, M., Nakayama, Y., Sader, J.E., & Jarvis, S.P., (2005). Quantitative measurement of solvation shells using frequency modulated atomic force microscopy. *Nanotechnology*, Vol. 16, No. 3, (January 2005), pp. (S49-S53), 0957-4484

Vázquez, J., Rivera, M.A., Hernando, J., & Sánchez-Rojas, J.L. (2009). Dynamic response to low aspect ratio piezoelectric microcantilevers actuated in different liquid environments. *J. Micromech. Microeng.*, Vol. 19, No. 1, (January 2009), pp. (1-9), 0960-1317

Verdaguer, A., Sacha, G.M., Bluhm, H., & Salmeron, M. (2006). Molecular structure of water at interfaces: wetting at the nanometer scale. *Chem. Rev.,*Vol. 106, (March 2006), pp. 1478-1510

Yamamoto, S.I., Yamada, H., & Tokumoto, H. (1997). Precise force curve detection system with a cantilever controlled by magnetic force feedback. *Review of Scientific Instruments*, Vol. 68, No. 11, (August 1997), pp. (4132-4136)